Steel and Composite Structures, *Vol*. *26*, *No*. *3* (*2018*) *361-373*
DOI: https://doi.org/10.12989/scs.2018.26.3.361

Numerical study of the cyclic behavior of steel plate shear wall systems (SPSWs) with differently shaped openings

Mustafa M. Ali*, S.A. Osman, O.A. Husam and Ahmed W. Al-Zand

Department of Civil and Structural Engineering, *Faculty of Engineering and Built Environment*, *Universiti Kebangsaan Malaysia* (*UKM*), *43600 Bangi*, *Selangor*, *Malaysia*

(*Received January 30, 2016, Revised August 25, 2017, Accepted December 2, 2017*)

Abstract. This paper presents the development of finite element (FE) models to simulate the behavior of diagonally stiffened steel plate shear wall systems (SPSWs) with differently shaped openings subjected to a cyclic load. This walling system has the potential to be used for shear elements that resist lateral loads in steel-framed buildings. A number of ½-scale one-story buildings that were un-stiffened, stiffened and stiffened with opening SPSWs are modeled and simulated using the finite element method based on experimental data from previous research. After validating the finite element (FE) models, the effects of infill plate thickness on the cyclic behavior of steel shear walls are investigated. Furthermore, triple diagonal stiffeners are added to the steel infill plates of the SPSWs, and the effects are studied. Moreover, the effects of a number of differently shaped openings applied to the infill plate are studied. The results indicate that the bearing capacity and shear resistance are affected positively by increasing the infill plate thickness and by adding triple diagonal stiffeners. In addition, the cyclic behavior of SPSWs is improved, even with an opening in the SPSWs.

Keywords: steel plate shear wall systems (SPSWs); FE simulation; cyclic behavior; diagonal stiffeners; openings

1. Introduction

A developed form of a steel plate shear wall system (SPSW), consisting of triple diagonal stiffeners applied on the infill mild plate with an opening and HEB160 (European standard wide flange H steel sections) for beams and columns (as shown in Fig. 1) ((a) one of the developed form; (b) Alavi and Nateghi 2012) has the potential to be applied as a lateral load resisting element in buildings with steel structures. The idea of this kind of SPSWs is based on the widely used multi-floor steel structures using SPSWs as studied by Hosseinzadeh and Seddighi (2014), Bruneau *et al*. (2011), Guo *et al*. (2011), Vatansever and Yardimci (2011), Kalali *et al*. (2015) which are especially important in areas of high seismic risk. Such SPSWs possess a good feature as Mojtahedi and Nourani (2015), Chatterjee *et al*. (2015), Alavi and Nateghi (2012) mention before, it is easy to add an opening to their infill plate. The purpose of the opening is for utilities to go through and meet the architectural aims and/or structural purpose of the system. Recent research on un-stiffened steel plate shear walls with openings have shown that their shear strength and stiffness are reduced due to the openings in the infill plate as studied by Salam and Wan Badaruzzaman (2015), which may not be acceptable in the design stage. This problem has prompted researchers to seek solutions for reducing the unwanted effects of openings on the structural and cyclic behavior of steel plate shear walls and that's shown by Hosseinzadeh and Tehranizadeh (2012). The connection between all parts (columns, beams, infill plate and stiffeners) of an SPSW is a tie (full welded) connection.

To improve the buckling capacity and lateral load bearing capacity, the global buckling of the infill steel plate should be restrained by using appropriate diagonal stiffeners at the infill steel plate. The suppression of global buckling and the enhancement of the buckling load will guarantee yielding of the infill steel plate prior to failure of the wall system.

The general behavior of SPSWs was demonstrated by Alavi and Nateghi (2013). In this paper, the nonlinear finite element computer program ABAQUS is used for simulations (Hibbitt and Sorensen 2002), and the results are validated by experimental results. To verify the ability of ABAQUS to analyze the behavior of SPSWs, three models were analyzed. A comprehensive parametric FE study was carried out to investigate the influence of triple diagonal stiffeners, as well as different shapes and locations of openings on the shear load-displacement response and ultimate lateral load capacity of SPSWs under cyclic loading.

2. Description of the finite element models

A steel plate shear wall with a central perforation and diagonal stiffeners was experimentally tested by Alavi and Nateghi (2013). Three models of ½-scaled single-story SPSWs, each with 2 m width and 1.5 m height, were used

*Corresponding author, Professor,
E-mail: mma1416@yahoo.com
[a] Ph.D.
[b] Ph.D. Student

ISSN: 1229-9367 (Print), 1598-6233 (Online)

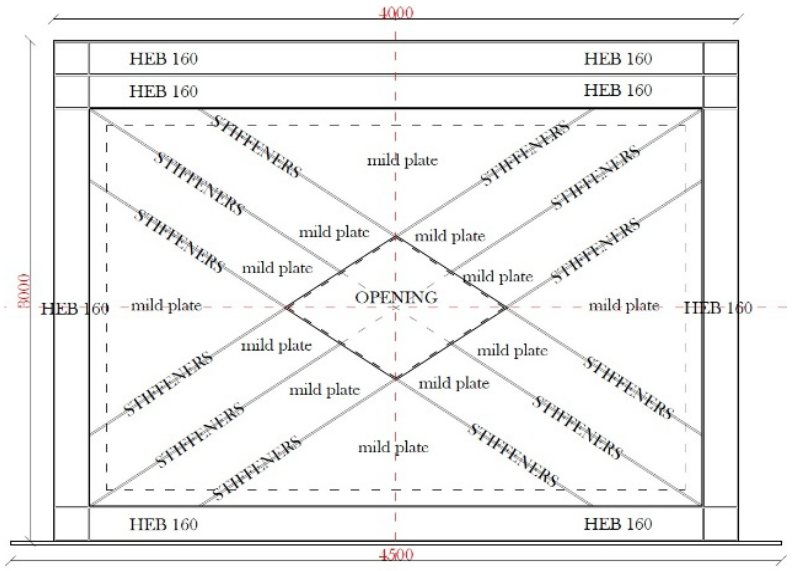

(a) A developed form of triple diagonal stiffeners applied on the infill mild plate of an SPSWs with rhombic opening

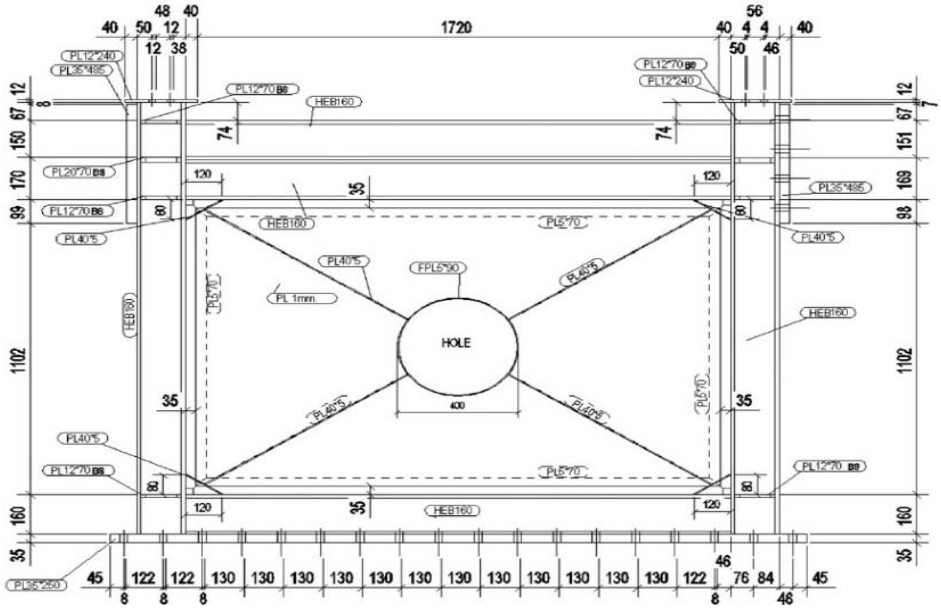

(b) Alavi and Nateghi (2012)

Fig. 1 A developed form and the origin sample of (SPSWs)

for the experimental program. The width to height ratio of the SPSW was 1.33, while the actual size of the shear wall was 4 m wide and 3 m high (a typical story height). The boundary elements were made of the standard profile section HEB160 (HEB beams, European standard wide flange H beams) and the infill mild steel plate thickness was 0.8 mm for the 1st and 2nd SPSWs and 1.0 mm for the 3rd SPSW, as shown in Table 1. All beam-to-column joints were full moment connections, made with an E7018 type electrode. The top of each specimen had double HEB160 steel sections connected along their flanges by welding. The first SPSW specimen, as shown in Fig. 2, was un-stiffened and thus used as the 1st control model. The mechanical properties of the steel materials, as measured with tension coupon tests in accordance with ASTM A370-05, are shown in Table 2. The second SPSW control model is shown in Fig. 3; it has diagonal stiffeners, measuring 40 mm × 4 mm and used in combination with edge stiffeners (40 mm × 4 mm), on both sides. The third SPSW control model was stiffened with two-sided diagonal and edge stiffener plates (40 mm × 5 mm) and contained a circular opening in the center, as shown in Fig. 4. The diameter of the circular opening was 400 mm, corresponding to 1/3 of the wall depth. The circular opening was stiffened by a ring-shaped stiffener plate measuring 90 mm × 5 mm. The diagonal stiffeners were located between the infill plate rim and the ring shape stiffeners, and connected to each other by welds.

To check the validity of the FE modeling using the ABAQUS/CAE (FE) software, models identical to the SPSWs used in the experimental study, with length (L) 2000 mm, and height (H) 1500 mm (1/2 scale), were used. Figs. 5(a), (b) and (c) show the SPSW models after meshing.

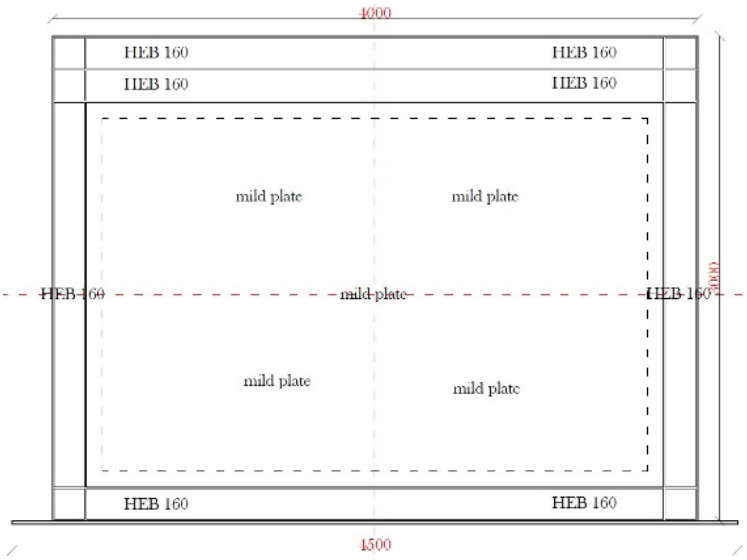

Fig. 2 1st control model

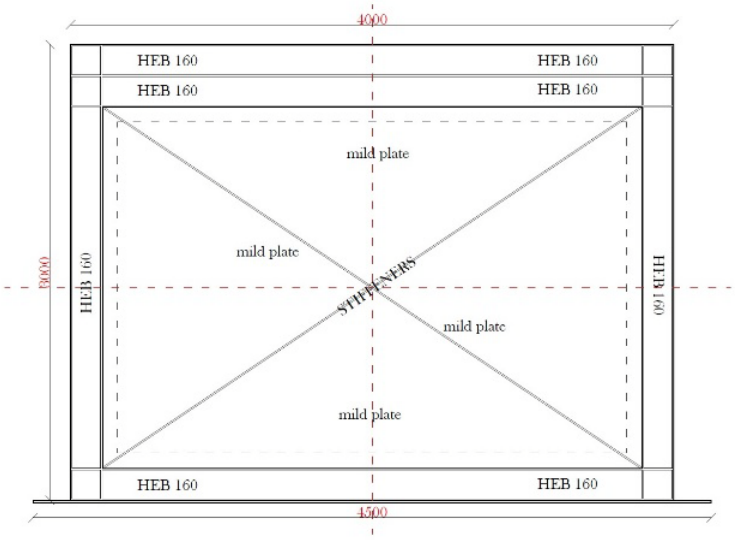

Fig. 3 2nd control model

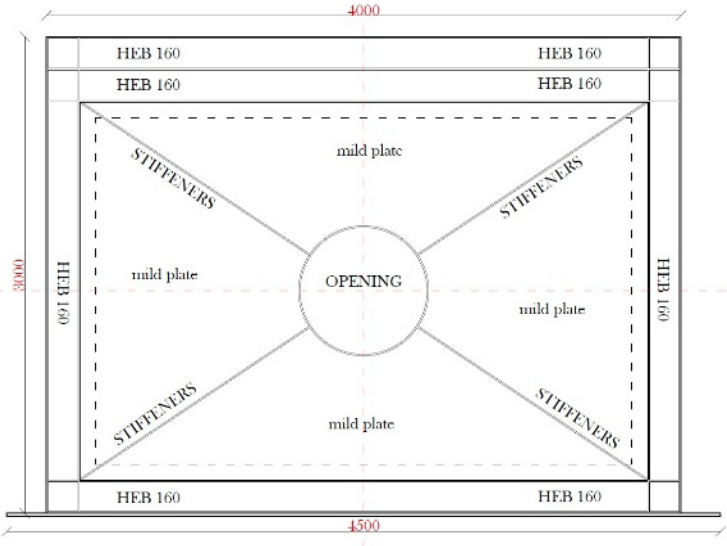

Fig. 4 3rd control model

Table 1 The control models table

Model No.	Frame Sec.	Infill plate THK	Stiffener plate THK	Opening	Opening stiffeners
1st control model	HEB160	0.8 mm	None	None	None
2nd control model	HEB160	0.8 mm	4 mm	None	None
3rd control model	HEB160	1.0 mm	4 mm	Circular 400 mm Dia.	5 mm

Table 2 Mechanical properties of steel materials

Steel material	Elastic modulus (MPa)	Static yield (MPa)	Static ultimate (MPa)	Yield strain (%)	Hardening strain (%)	Ultimate strain (%)	Rupture strain (%)
HEB 160 frame section	2.06E+05	340	450	0.17	1.8	14.4	16.2
Opening stiffeners plate	2.05E+05	340	470	0.17	3.06	20.5	22.3
Diagonal stiffeners plate	2.05E+05	460	550	0.22	2.67	19.1	20.8
Main mild infill plate	2.04E+05	280	500	0.14	0.3	21.6	27.0

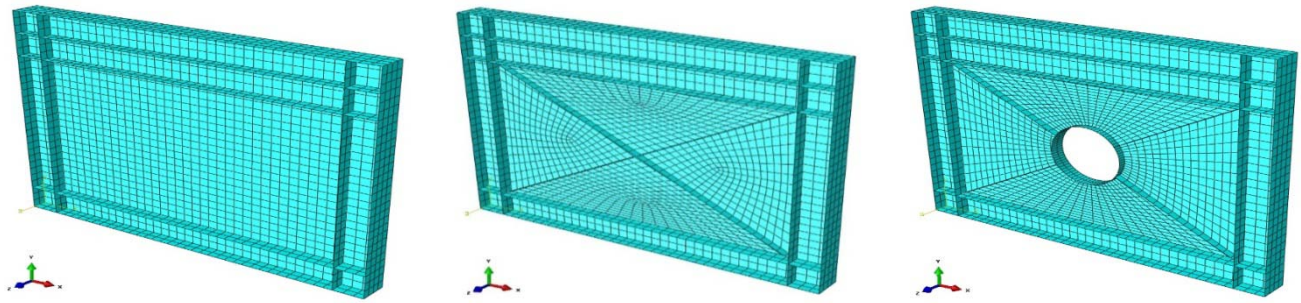

(a) Model 1 (b) Model 2 (c) Model 3

Fig. 5 FE modeling of control models (ABAQUS/CAE)

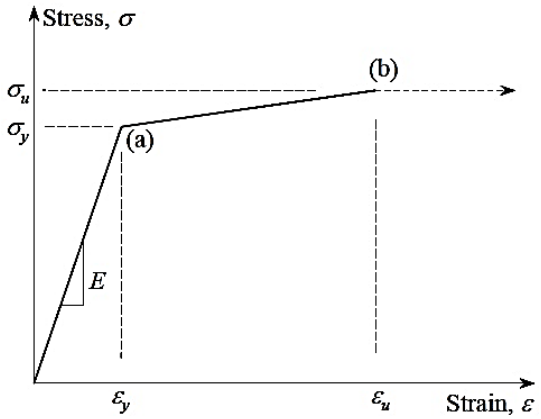

Fig. 6 Bilinear stress-strain relationship for steel (ABAQUS/CAE)

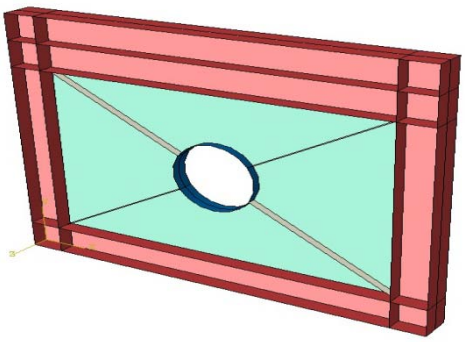

Fig. 7 Parts of SPSW (ABAQUS/CAE)

The material properties used for both the infill plates and the boundary frame members (beams and columns) were taken from the tension coupon test results reported by Alavi and Nateghi (2013), as shown in Table 2. All models were assumed to consist of plastic-bilinear material, with stress-strain behavior, as shown in Fig. 6.

The FE models were assembled from four parts, including the frame, which consisted of two columns, double beams at the top of the SPSW and a single beam at the base of the SPSW, the infill steel plate, the diagonal stiffeners and the opening stiffeners (Fig. 7). All parts were connected to each other by tie connections, which are intended to represent the welds.

A convergence study on the half-scale models shown in Fig. 5 was carried out to determine the appropriate mesh size for the model. Four-node shell elements were used and mesh sizes of 120 mm, 100 mm, 60 mm, 50 mm, 40 mm and 30 mm were simulated sequentially. It can be concluded from Fig. 8 that the differences between the 50 mm, 40 mm and 30 mm mesh sizes were negligible. Therefore, the 50 mm model is adopted here for all SPSWs.

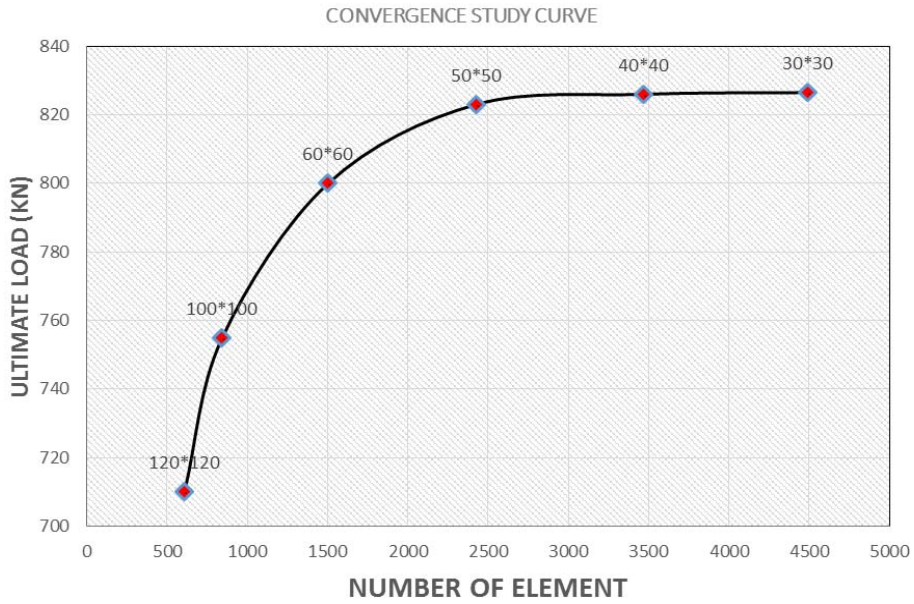

Fig. 8 Results of convergence study

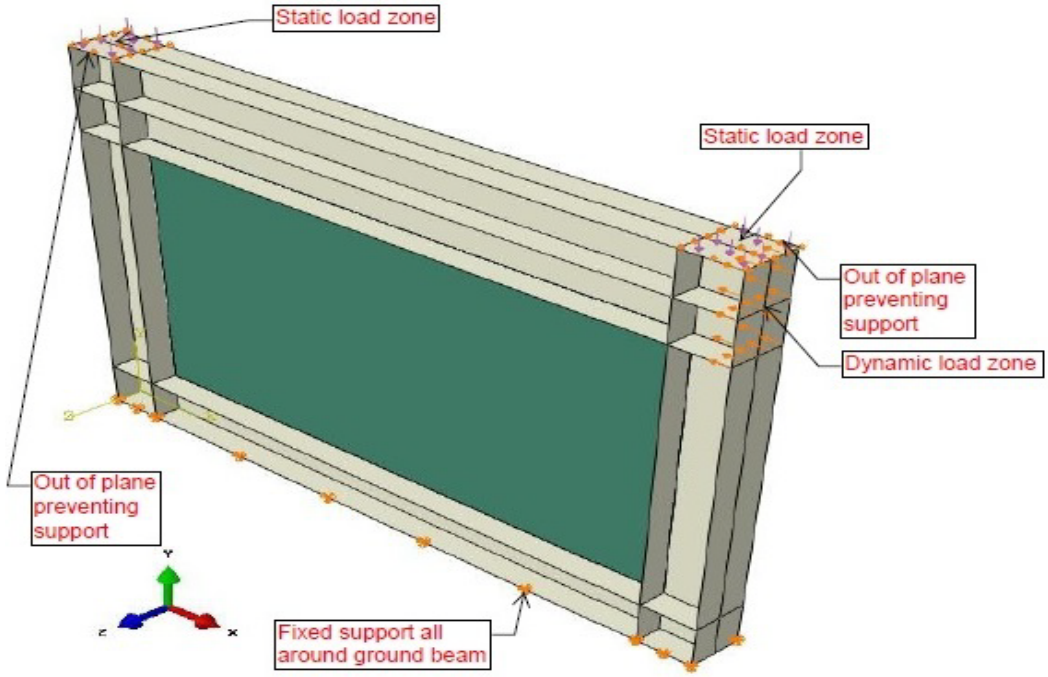

Fig. 9 Boundary condition in ABAQUS

The boundary condition used for the SPSWs was identical to that of the specimen used in the laboratory test. The bottom edge and the tops of both the vertical portions and the base of each column were fixed, as shown in Fig. 9. The cyclic load was applied based on the test protocol 1992 ATC-24. The loading history consisted of stepwise increasing deformation cycles, as shown in Fig. 10.

The validity of three the SPSW control models was verified by comparing the results of the FE simulation with existing experimental results from Alavi and Nateghi (2013). For all control models, the finite element solution is in acceptable agreement with the experimental results throughout the entire range of loading. The verification result shows that the approximations are acceptable and the percent difference between the results is approximately 6.9%, confirming that the suggested FE model is appropriate to test the cyclic behaviors of the SPSWs adopted in this paper. Figs. 11(a), (b) and (c) show the comparison of the resulting curves. Moreover, due to hardening model and perfect environment of FE models combined, which led to more stiffness acting, it can be noted that, there is no full matching observed between cycles and loops of the experimental and FE hysteresis curves.

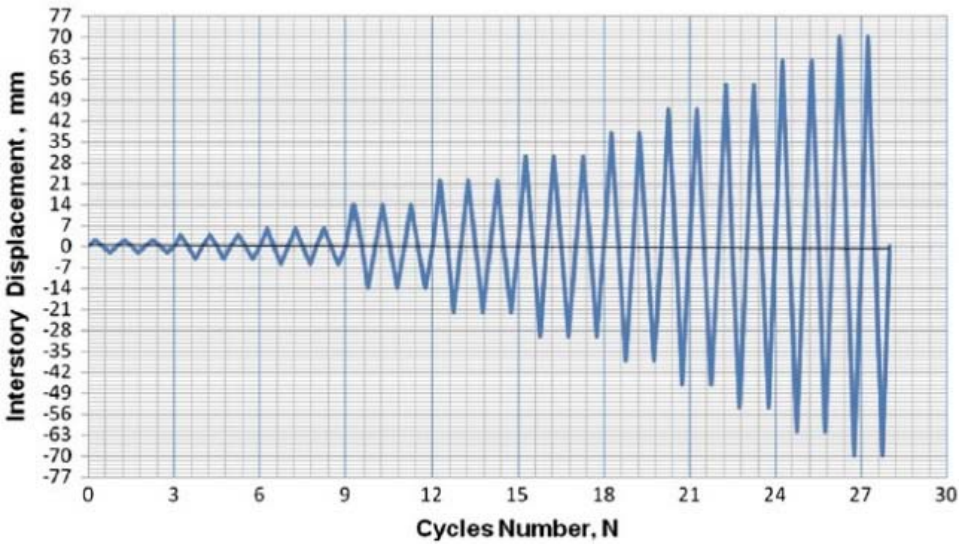

Fig. 10 Loading history based on steel (Source: ATC-24 cyclic load test protocol 1992)

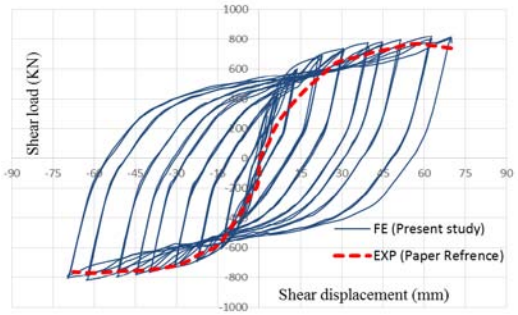

(a) 1st control model

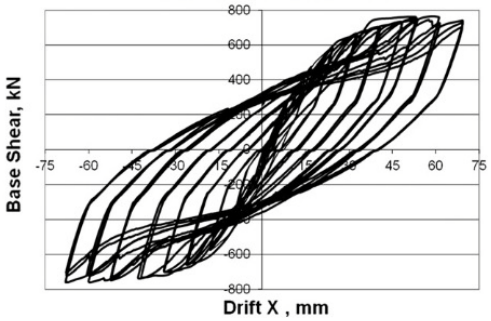

Hysteresis curves of the specimen from experimental test (Alavi and Nateghi (2013)

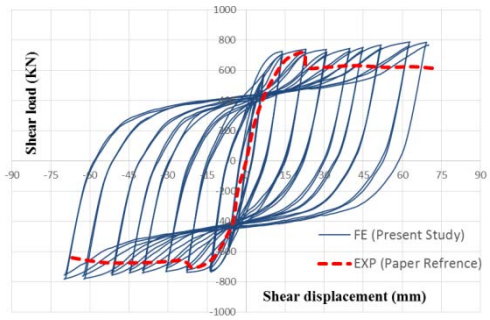

(b) 2nd control model comparison

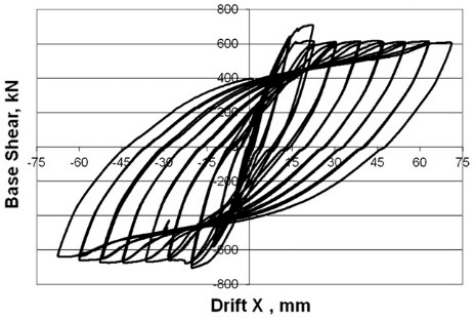

Hysteresis curves of the specimen from experimental test (Alavi and Nateghi (2013)

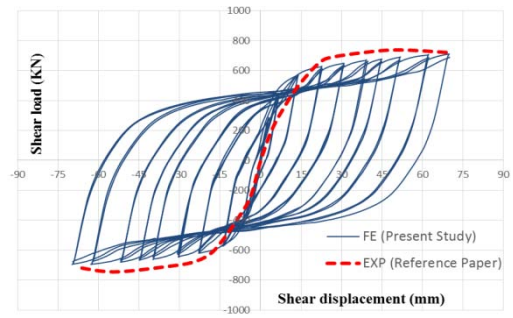

(c) 3rd control model comparison

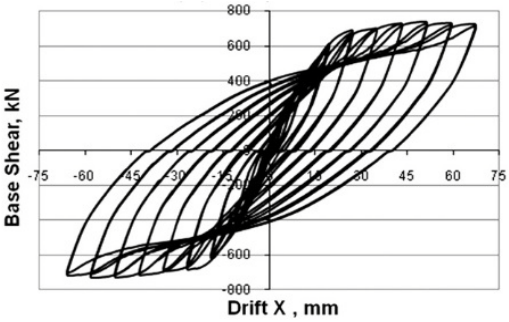

Hysteresis curves of the specimen from experimental test (Alavi and Nateghi (2013)

Fig. 11 Comparison of hysteresis curves for control models and experimental specimens

Table 3 The parametric study modeling details

	Model No.	Frame Sec.	Infill plate thickness (mm)	Diagonal stiffeners	Offset distance for stiffeners	Diagonal stiffeners plate THK (mm)	Opening shape and location	Opening stiffeners THK (mm)
Effect of infill plate THK	Model 4	HEB160	1.5	None	None	None	None	None
	Model 5	HEB160	2.0	None	None	None	None	None
	Model 6	HEB160	2.5	None	None	None	None	None
	Model 7	HEB160	3.0	None	None	None	None	None
Effect of stiffeners	Model 8	HEB160	0.8	Triple	350	4	None	None
	Model 9	HEB160	0.8	Triple	200	4	None	None
	Model 10	HEB160	0.8	Triple	100	4	None	None
Effect of different shapes and locations of openings	Model 13	HEB160	0.8	Triple	200	4	Central circle	4
	Model 14	HEB160	0.8	Triple	350	4	Central rhombic	4
	Model 15	HEB160	0.8	Triple	200	4	Central rectangular	4
	Model 16	HEB160	0.8	Triple	200	4	2 triangles on sides	4
	Model 17	HEB160	0.8	Triple	200	4	2 triangles on top and bottom	4
	Model 18	HEB160	0.8	Triple	200	4	4 triangles	4

3. Parametric study and analyses

To investigate further the effects of using different parameters in the SPSWs, a series of parametric studies were carried out. The parameters considered were the thickness of the main mild plate, the stiffeners, and the shape and number of openings. In each numerical test, only the specified parameter is varied, while all other parameters were kept constant to determine the effects of the considered parameter on the cyclic behavior of the SPSWs. Table 3 shows the modeling details of the parametric study.

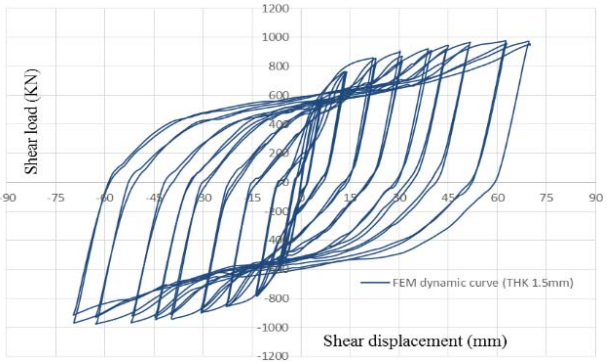

Fig. 12 Model 4 curve

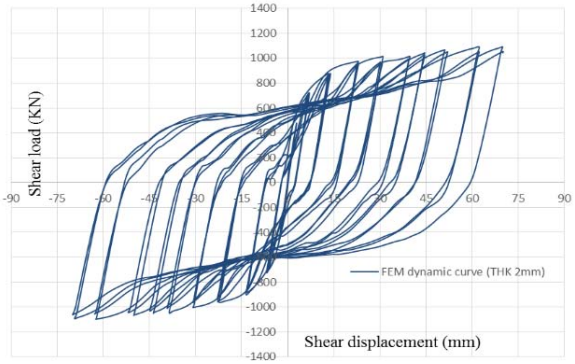

Fig. 13 Model 5 curve

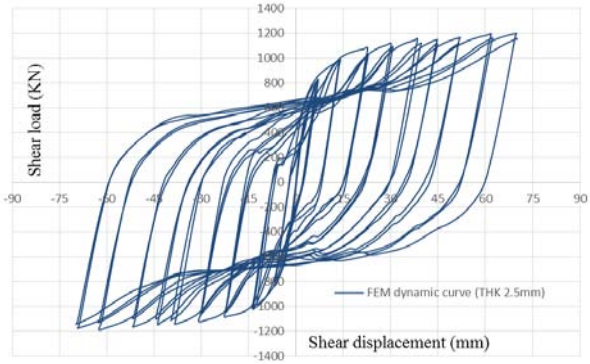

Fig. 14 Model 6 curve

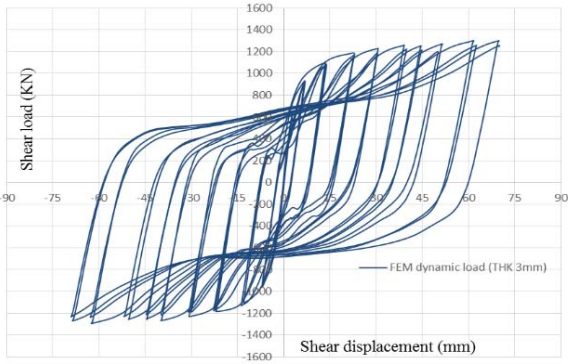

Fig. 15 Model 7 curve

3.1 Effect of infill mild steel plate thickness

To determine the effect of infill plate thickness, models 4, 5, 6 and 7, were simulated and analyzed according to Table 3. The results obtained from the finite element analysis are given as load-displacement curves and are shown in Figs. 12, 13, 14 and 15. It is evident that the ultimate load increases when the thickness of the infill steel plate is increased.

3.2 Effect of stiffeners

Figs. 16, 17 and 18 show the effect of triple stiffeners on the dynamic behavior of SPSWs, where each diagonal direction has a different offset distance between the stiffeners, as shown in Table 3. It is clear that both the ultimate load and the shear load capacity increase when the number of stiffeners is increased from 1 to 3. It should also be noted that the displacement was different for these three models, due to the high stiffness caused by the addition of triple stiffeners, which affect the ductility behavior of SPSWs directly, as shown in Fig. 25. Moreover, as the offset distance of the stiffeners is reduced, the shear load capacity tends to rise. For model 8, with a 350 mm offset distance, the infill plate deformed noticeably more at the edge than at the center, which led to earlier failure. For model 9, with a 200 mm offset distance, the shear stress increased and started to spread into the infill plate edge, though the infill plate center deformed more than in the other models. For model 10, with a 100 mm offset distance, the shear stress increased even more and the infill plate became stiffer, which led to a higher concentration of the

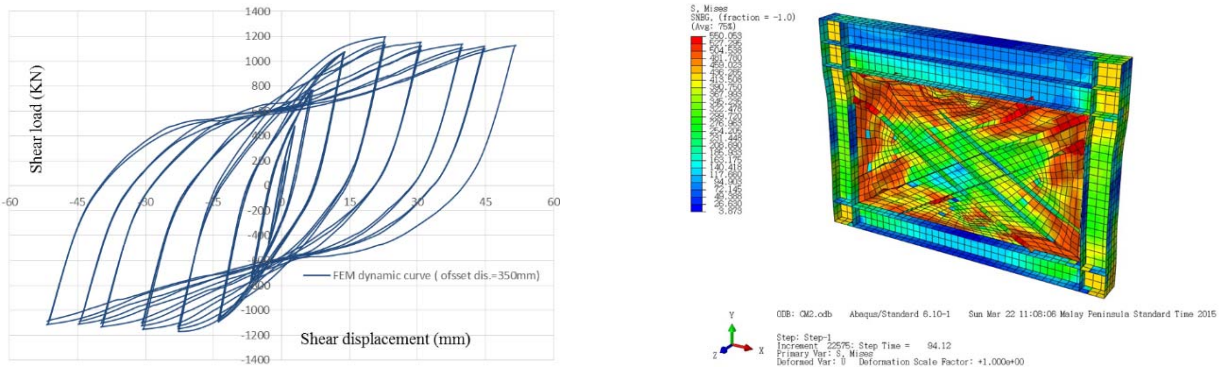

Fig. 16 Model 8 curve and deformed specimen

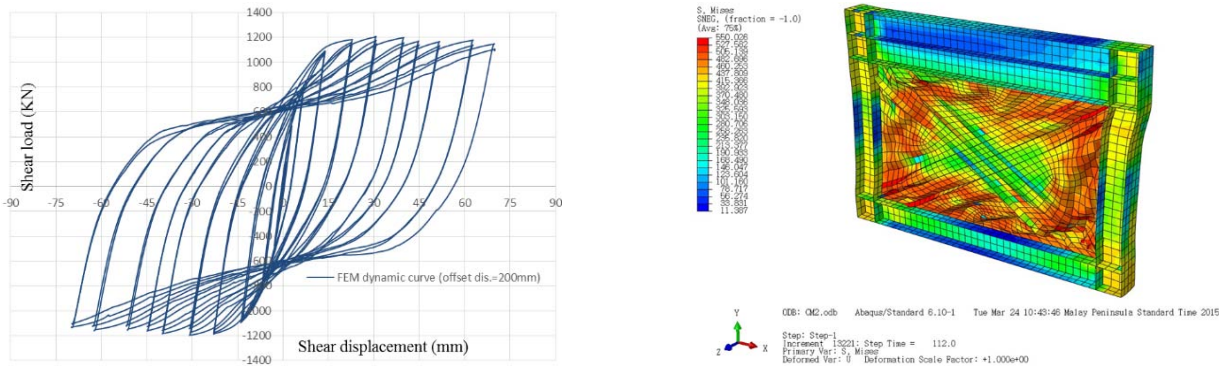

Fig. 17 Model 9 curve and deformed specimen

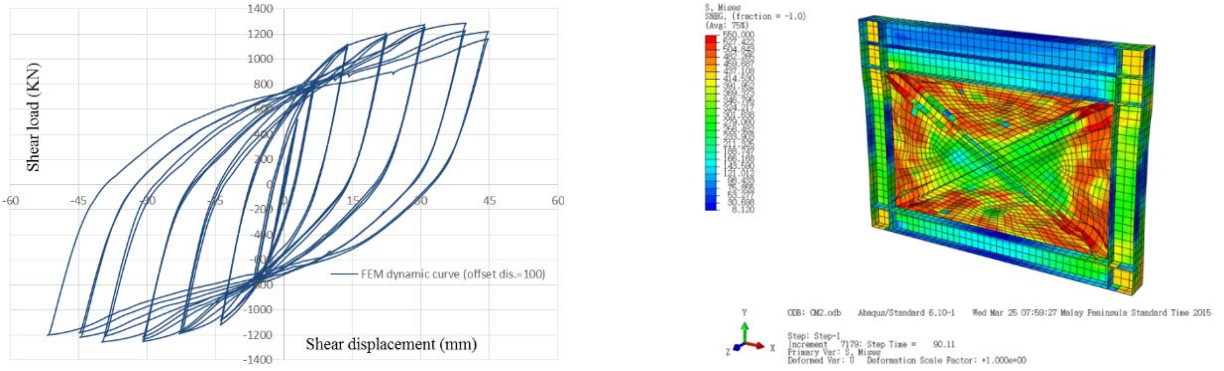

Fig. 18 Model 10 curve and deformed specimen

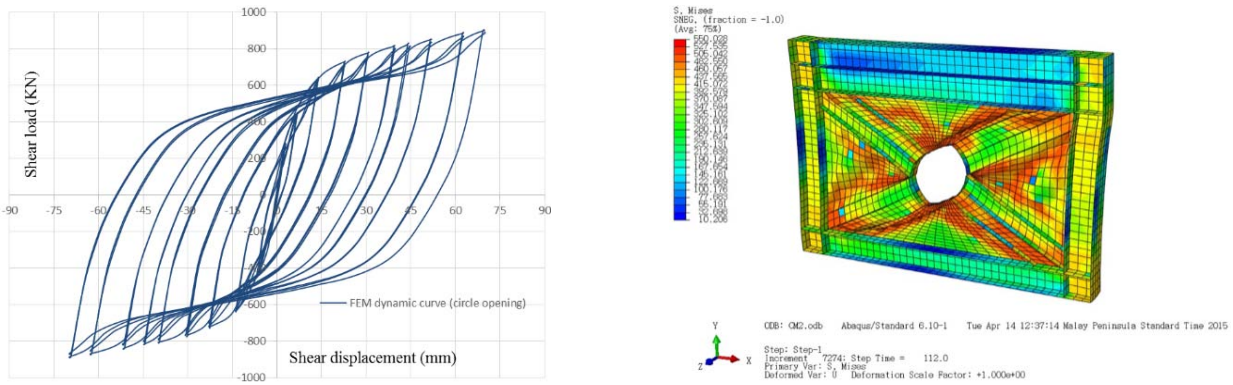

Fig. 19 Model 13 curve and deformed specimen

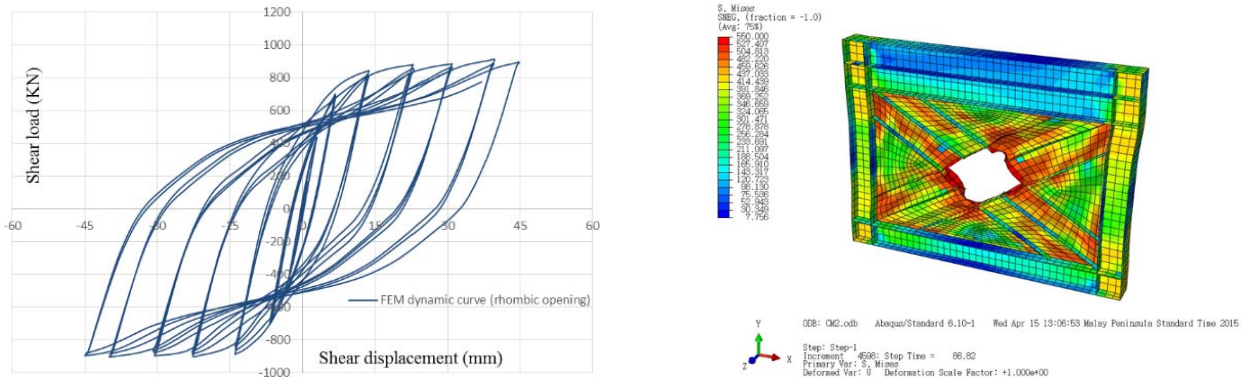

Fig. 20 Model 14 curve and deformed specimen

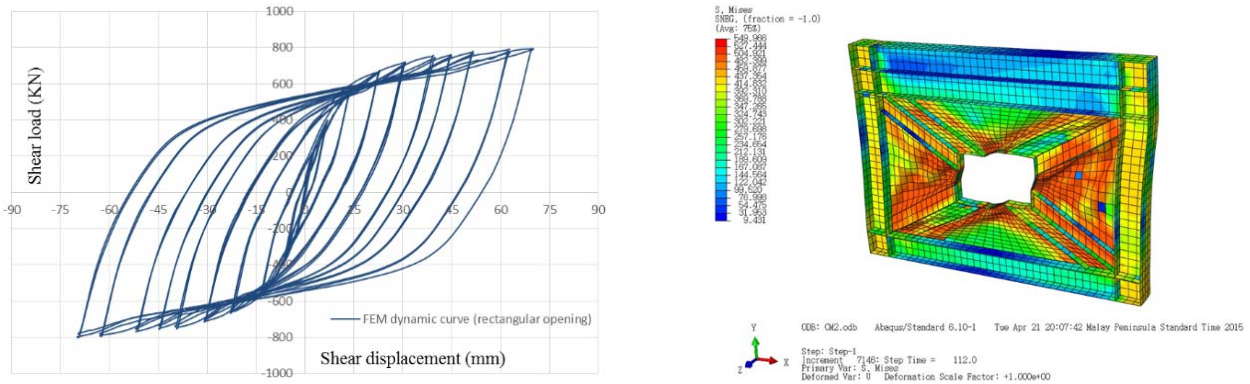

Fig. 21 Model 15 curve and deformed specimen

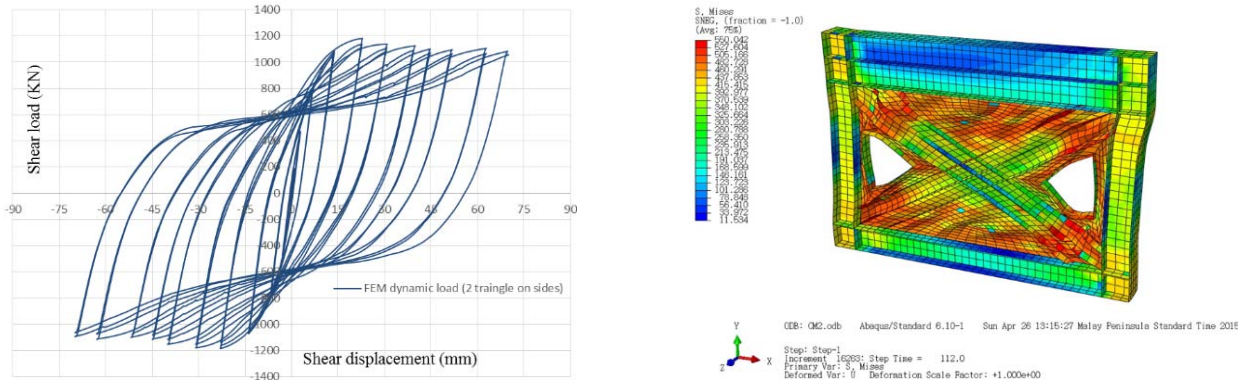

Fig. 22 Model 16 curve and deformed specimen

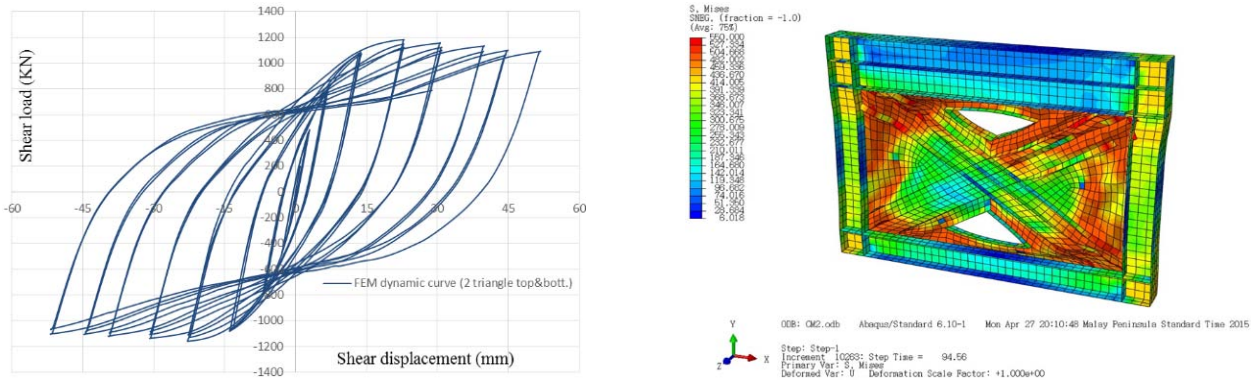

Fig. 23 Model 17 curve and deformed specimen

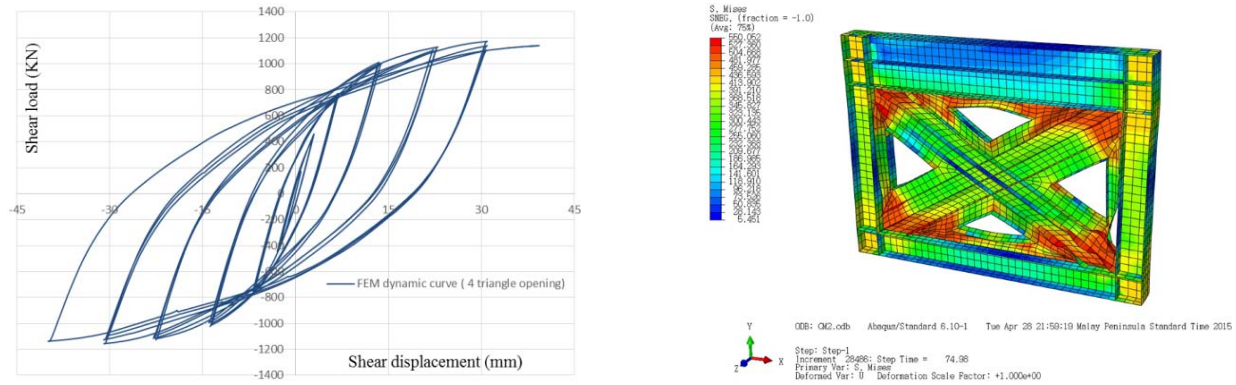

Fig. 24 Model 18 curve and deformed specimen

shear stress at the infill plate edge and earlier failure. The cyclic load improvement ratios are shown in Fig. 25.

3.3 Effect of multi shapes and location of opening

In this section, models with differently-shaped openings were simulated and analyzed. It should be noted that the use of circular and rectangular openings cuts or breaks all stiffeners at the center of the SPSWs. On the other hand, a rhombic opening will cut/break 1/3 of the stiffeners. It should be noted also that the height of the shapes was 1/3 of the infill steel plate. Therefore, a triangular shape was suggested and designed in such a way to not affect the extension of the stiffeners. The offset distance of the rhombic opening was 350 mm to keep 2/3 of the stiffeners and to create a suitably-sized opening at the center of the

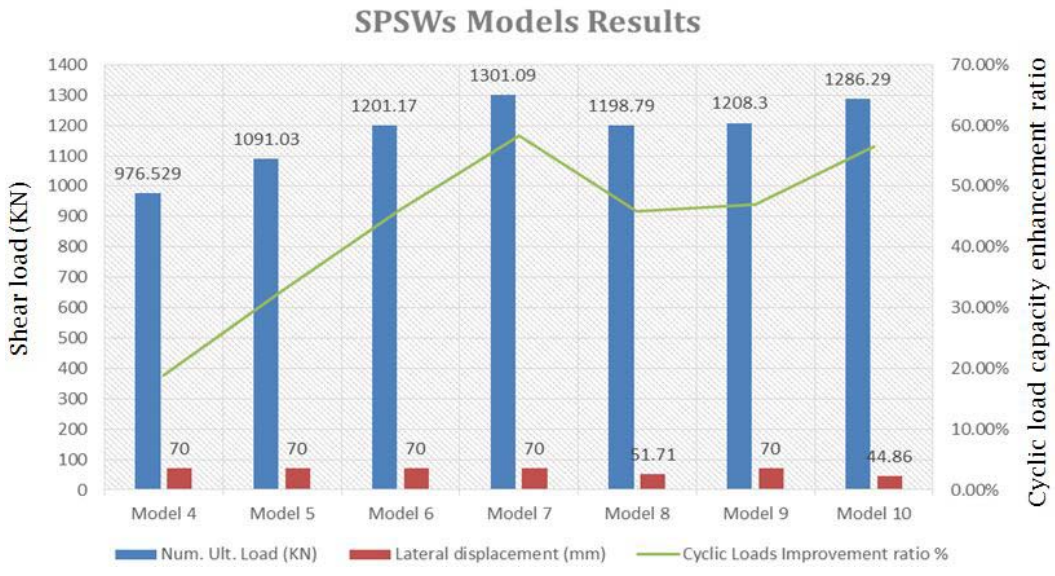

Fig. 25 SPSWs models result

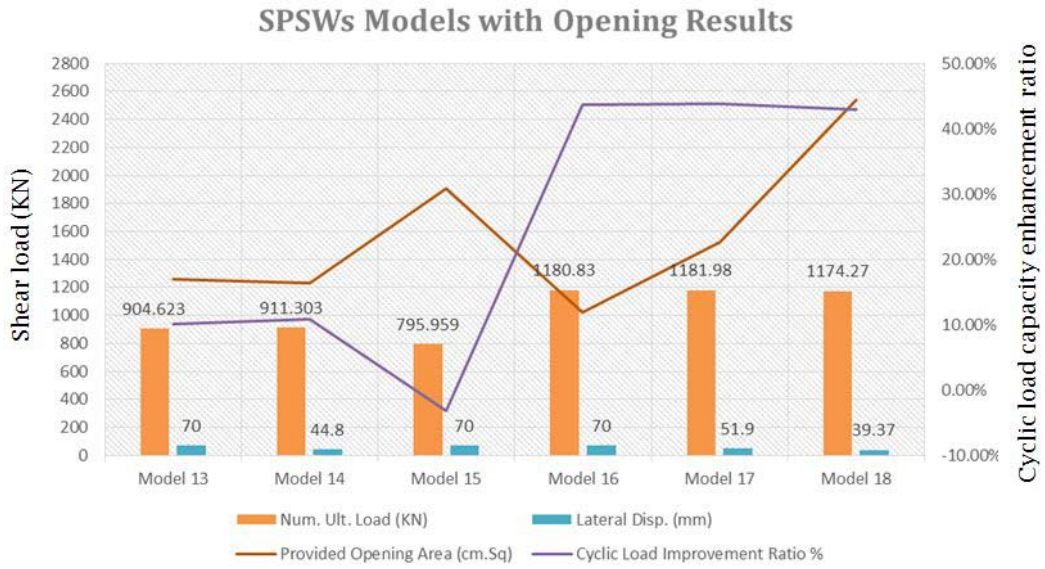

Fig. 26 SPSWs models with openings result

SPSWs. The rest of the models used a 200 mm opening because only models with this size achieved the required lateral displacement, as shown in Figs. 19, 20 and 21. It should be noted that only the circular shape was used in the experimental test.

It is clear that, for model 13, with the circular opening, the stress was distributed on the four parts of the infill plate. Model 14, with the rhombic opening, shows stress concentrated more on the edge of the opening and between the stiffeners and less stress distributed on the four parts. Model 15, with the rectangular opening, shows that the stress was divided into four parts, with higher concentrations on the side parts.

Furthermore, it can be concluded that the triple diagonal stiffeners have remedied the weakness in the total structural behavior, which was caused by the openings that kept the cyclic load capacity quite similar to the un-stiffened mild type.

From the hysteresis loop curves for models 13 and 14, it can be noted that the maximum shear load capacity was increased because of the circular and rhombic openings and the three stiffeners in each diagonal direction. Fig. 20 shows that model 14 achieved less lateral displacement because the rhombic opening allowed for 2/3 of the stiffeners to remain, which led to stiffer behavior and earlier failure. On the other hand, model 15 showed a slight decrease in bearing capacity, as compared to the 1st control model, due to the large size of the rectangular opening. The cyclic load improvement ratios are shown for each of the models with openings in Fig. 26.

Furthermore, some design cases require more than a single opening, and the results of this study suggest the idea of having two triangular openings either on top and bottom or on the sides. An alternative would be four openings also at the top, bottom and sides.

Figs. 22, 23 and 24 show the effect of using a triangular opening on the dynamic behavior of SPSWs. It is very clear from the results for models 16, 17 and 18 that the shear load capacity is increased when using three stiffeners in each diagonal direction with two and four triangular openings. It should also be noted that the results show different lateral displacements for each of these three models, as shown in Fig. 26.

The result for model 16 shows that the location of the opening did not affect the ductility behavior of the SPSWs since the type of opening can be defined by its configuration or by being adjacent to the columns/beams of the panel. The load stress was resisted by the frame and stiffeners. Model 17 shows that the opening location directly affected the ductility behavior because the opening and the cyclic load were located on the same axis. Furthermore, the load stress started from the frame and then directly reached the opening location. Model 18 shows that the four openings had significant influence on the ductility behavior, which caused the stress to concentrate on the corners, leading a reduction in ductility, earlier failure and reduced bearing capacity. Fig. 25 shows the cyclic load improvement ratio, which is the percentage of enhancement in maximum cyclic load capacity and is obtained by computing the percent difference between the maximum cyclic load capacity of the 1st control model and each one of the parametric models, divided by the maximum cyclic load capacity of the 1st control model. It is expressed as follows

$$IR = \frac{P\ model - P\ cm}{P\ model} * 100\% \quad (1)$$

where IR is the improvement ratio, $P\ model$ is the maximum cyclic load capacity of the model in question and $P\ cm$ is the maximum cyclic load capacity of the 1st control model. The ultimate load, lateral displacement, opening area and cyclic load capacity enhancement ratio for all SPSWs with openings are shown in Fig. 26.

4. Ductility

For convenience in the subsequent analysis, the ductility

Table 4 The ultimate displacement at failure, displacement at yielding and ductility coefficient values

Model No.	Δu value	Δy value	μ value
Model 4	68.87	2.01	34.18
Model 5	69.27	3.57	19.40
Model 6	69.70	3.25	21.43
Model 7	69.32	3.74	18.52
Model 8	22.94	2.40	9.56
Model 9	30.13	2.75	10.97
Model 10	30.32	2.57	11.81
Model 13	69.24	3.87	17.89
Model 14	39.74	2.81	14.16
Model 15	69.50	2.92	23.79
Model 16	22.88	2.30	9.96
Model 17	22.65	2.84	7.98
Model 18	30.73	2.85	10.79

coefficient (μ) is defined herein to quantify the ductility of diagonally stiffened SPSWs with different shapes of opening subjected to a cyclic load. It is expressed as follows

$$\mu = \frac{\Delta u}{\Delta y}$$

where Δu is the ultimate displacement at failure, and Δy is the displacement at yielding.

Table 4 shows the ultimate displacement at failure, displacement at yielding and ductility coefficient values for all FE models.

Fig. 27 shows the ductility coefficient (μ) for all models. It is evident that in group (a), μ decreases with increasing infill plate thickness, due to increasing stiffness caused by the thicker infill plate. Group (b) shows a small effect due to the clear distance between diagonal stiffeners, which is attributable to the fact that the stiffeners have the same effect on the same zone area of the infill plate. Group (c) shows that the models with central openings are more

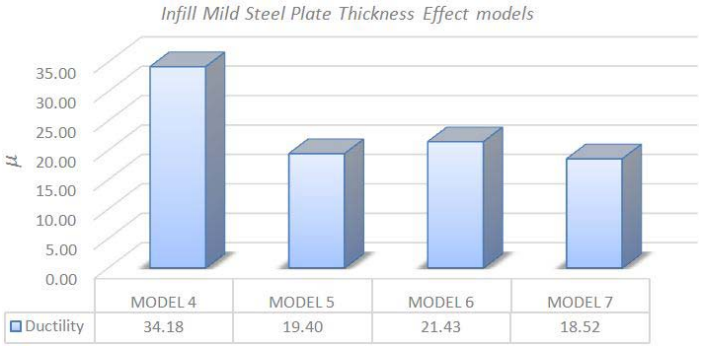

(a) Effect of infill mild steel plate thickness

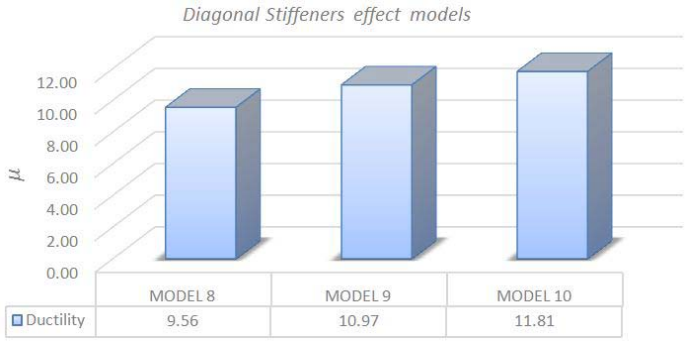

(b) Effect of diagonal stiffeners

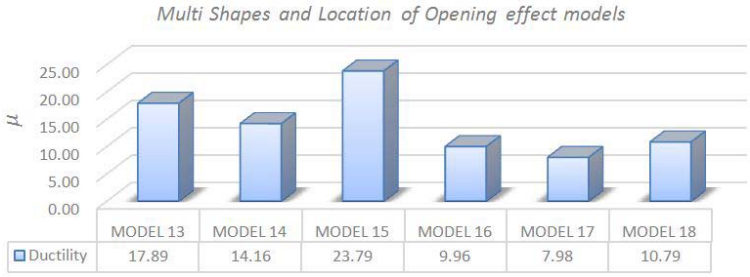

(c) Effect of shape and location of opening

Fig. 27 Effect of infill mild steel plate thickness, diagonal stiffeners and openings on the value of ductility

ductile than others because this location of opening tends to distribute the stress over the whole infill plate area. Generally, μ decreases with increasing opening ratio.

5. Conclusions

This paper presents a finite element study on multi-purpose openings in a SPSWs; these openings allow access through the shear wall without considerable negative effects either on the strength or stiffness under cyclic loading. To that end, thirteen half-scale, single-story models of steel plate shear walls with different details were modeled and analyzed.

The numerical results have shown the following:

- The specimens had stabilized hysteretic loops.
- The use of triple diagonal stiffeners along with the opening was an effective and applicable adjustment to the infill plate.
- The structural properties of the triple diagonally stiffened shear wall with openings are near to the un-stiffened mild type or are even improved in some areas.
- In view of these results, it is concluded that the triple diagonally stiffened shear wall with openings is an influential lateral load resisting system.
- Triple diagonal stiffening is an adequate strengthening solution for shear walls with openings.
- The location of the openings had different effects on the ductility due mostly because of the proximity to the diagonal corrugated waves of the infill plate, which are caused by the applied cyclic load and the diagonal stiffeners.
- While the effects of welding and imperfections on the cyclic behavior have not been experimentally tested for these new models, these are expected to have an insignificant effect due to the frame durability and thinning of the infill plate, which causes fracture to occur in the infill plate before occurring on the welding line during loading.

Acknowledgments

The authors wish to express appreciation and support given by the Department of Civil & Structural Engineering and the Universiti Kebangsaan Malaysia through grant Arus Perdana (AP-2015-011).

References

AISC (2010), Specification for StructuralSteel Buildings; Chicago, IL, USA.

Alavi, E. and Nateghi, F. (2012), "Experimental study of diagonally stiffened steel plate shear walls", *J. Struct. Eng.*, **139**(11), 1795-1811.

Alavi, E. and Nateghi, F. (2013), "Experimental study on diagonally stiffened steel plate shear walls with central perforation", *J. Constr. Steel Res.*, **89**, 9-20.

Barkhordari, M., Asghar Hosseinzadeh, S. and Seddighim M. (2014), "Behavior of steel plate shear walls with stiffened full-height rectangular openings", *Asian J. Civil Eng.* (*BHRC*), **15**, 741-759.

Bruneau, M., Uang, C.-M. and Sabelli, S.R. (2011), *Ductile Design of Steel Structures*, McGraw Hill Professional.

Chatterjee, A.K., Bhowmick, A. and Bagchi, A. (2015), "Development of a simplified equivalent braced frame model for steel plate shear wall systems", *Steel Compos. Struct., Int. J.*, **18**(3), 711-737.

Chen, S.-J. and Jhang, C. (2011), "Experimental study of low-yield-point steel plate shear wall under in-plane load", *J. Constr. Steel Res.*, **67**(6), 977-985.

Feizi, M.G., Mojtahedi, A. and Nourani, V. (2015), "Effect of semi-rigid connections in improvement of seismic performance of steel moment-resisting frames", *Steel Compos. Struct., Int. J.*, **19**(2), 467-484.

Guo, Y., Zhou, M., Dong, Q. and Wang, X. (2011), "Experimental study on three types of steel plate shear walls under cyclic loading", *Jianzhu Jiegou Xuebao* (*J. Build. Struct.*), **32**(1), 17-29.

Hibbitt, K. and Sorensen (2002), ABAQUS/CAE User's Manual: Hibbitt, Karlsson & Sorensen, Incorporated.

Hilo, S.J., Badaruzzaman, W.W., Osman, S.A., Al-Zand, A.W., Samir, M. and Hasan, Q.A. (2015), "A state-of-the-art review on double-skinned composite wall systems", *Thin-Wall. Struct.*, **97**, 74-100.

Hosseinzadeh, S. and Tehranizadeh, M. (2012), "Introduction of stiffened large rectangular openings in steel plate shear walls", *J. Constr. Steel Res.*, **77**, 180-192.

Kalali, H., Hajsadeghi, M., Zirakian, T. and Alaee, F.J. (2015), "Hysteretic performance of SPSWs with trapezoidally horizontal corrugated web-plates", *Steel Compos. Struct., Int. J.*, **19**(2), 277-292.

Krawinkler, H. (1992), *Guidelines for cyclic seismic testing of components of steel structures*, Applied Technology Council.

Standard ASTM E8/E8M (2009), Standard test methods for tension testing of metallic materials; ASTM International, West Conshohocken, PA, USA. DOI: 10.1520. E0008-E0008M-09

Vatansever, C. and Yardimci, N. (2011), "Experimental investigation of thin steel plate shear walls with different infill-to-boundary frame connections", *Steel Compos. Struct., Int. J.*, **11**(3), 251-271.

Wang, M., Yang, W., Shi, Y. and Xu, J. (2015), "Seismic behaviors of steel plate shear wall structures with construction details and materials", *J. Constr. Steel Res.*, **107**, 194-210.

Wong, M.Y., Shanmugam, N.E. and Osman, S.A. (2010), "Free vibration characteristics of horizontally curved composite plate girder bridges", *Steel Compos. Struct., Int. J.*, **10**(4), 297-315.

CC